A cost-effective process chain for thermoplastic microneedle manufacture combining laser micro-machining and micro-injection moulding

Gulcur, Mert; Romano, Jean-Michel; Penchev, Pavel; Gough, Tim; Brown, Elaine; Dimov, Stefan; Whiteside, Ben

DOI:
10.1016/j.cirpj.2021.01.015

Document Version
Peer reviewed version

Citation for published version (Harvard):
Gulcur, M, Romano, J-M, Penchev, P, Gough, T, Brown, E, Dimov, S & Whiteside, B 2021, 'A cost-effective process chain for thermoplastic microneedle manufacture combining laser micro-machining and micro-injection moulding', *CIRP Journal of Manufacturing Science and Technology*, vol. 32, pp. 311-321. https://doi.org/10.1016/j.cirpj.2021.01.015

A cost-effective process chain for thermoplastic microneedle manufacture combining laser micro-machining and micro-injection moulding

Mert Gülçür [a] (*), Jean-Michel Romano [b,c], Pavel Penchev [b], Tim Gough [a], Elaine Brown [a], Stefan Dimov [b], Ben Whiteside [a]

[a] Centre for Polymer Micro & Nano Technology, Faculty of Engineering and Informatics, University of Bradford, Bradford BD7 1DP, UK

[b] Department of Mechanical Engineering, School of Engineering, University of Birmingham, Edgbaston, Birmingham B15 2TT, UK

[c] IREPA LASER, Institut Carnot Mica, Boulevard Sébastien Brant, Illkirch, 67400, France

*Corresponding author: Dr. Mert Gulcur, m.gulcur@bradford.ac.uk

Postal address:

University of Bradford
Richmond Rd.
Polymer IRC,
Bradford
BD71DP
United Kingdom

All figures should be in colour in the online version.

ABSTRACT

High-throughput manufacturing of transdermal microneedle arrays poses a significant challenge due to the high precision and number of features that need to be produced and the requirement of multi-step processing methods for achieving challenging micro-features. To address this challenge, we report a flexible and cost-effective process chain for transdermal microneedle array manufacture that includes mould production using laser machining and replication of thermoplastic microneedles via micro-injection moulding (micromoulding). The process chain also incorporates an in-line manufacturing data monitoring capability where the variability in the quality of microneedle arrays can be determined in a production run using captured data. Optical imaging and machine vision technologies are also implemented to create a quality inspection system that allows rapid evaluation of key quality indicators. The work presents the capability of laser machining as a cost-effective method for making microneedle moulds and micro-injection moulding of thermoplastic microneedle arrays as a highly-suitable manufacturing technique for large-scale production with low marginal cost.

Keywords: microneedle arrays, micro-injection molding, laser micro-machining, process monitoring, data acquisition, polymer replication

HIGHLIGHTS

- A microneedle mould insert has been produced using laser micro-machining in less than 45 minutes.
- State-of-the-art micro-injection moulding has been used for replication of the microneedle cavities.
- An automated, bespoke measurement apparatus for the quality assessment of microneedles has been developed.
- Process data have been interrogated for in-line quality assurance of microneedle arrays.

Introduction

Transdermal microneedles are increasingly drawing attention from scientists and engineers due to their applications for drug delivery, body condition monitoring purposes and implementation in other medical technologies in recent years. Utilisation of microneedles for drug delivery has significant advantages, most notably, the transportation of larger molecules through the skin with minimally invasive (and pain-free) procedures as emphasised in a detailed review by Prausnitz (2004). Another significant benefit that stands out is the elimination of the need for healthcare professionals since the drug-coated or dissolvable microneedle patches can be self-administered by the patient as discussed in a more recent review by Prausnitz (2017). These advantages and a large variety of applications make the microneedle technology a promising and appealing research field, however, challenges remain regarding the high-volume manufacture of microneedle arrays. Obtaining a repeatable processes for replication of microneedle geometries, quality assurance and mould making are some of the more significant challenges in microneedle research (Tarbox et al. 2018; Juster et al. 2019; Evens et al. 2020).

Microneedles are micro-scaled and usually tapered protrusions that can be in conical, pyramidal, or cylindrical shapes with the following attributes:

1) A sharp tip to ensure good penetration of the structure through *stratum corneum* layer of the skin. Tip radii <5 μm are preferred, although <20 μm is deemed acceptable in many cases.
2) A suitable length to ensure the active ingredient is delivered to the target skin layer, but not sufficiently deep to contact nerve endings and cause pain. The height of the microneedles can vary between 100-1000 μm depending on the functionality.
3) A wider base/support structure for maintaining mechanical stability. These are typically of the order of 300-700 μm in diameter.

The small scale of each needle has the consequence that only very small payloads, fluid sampling volumes or electrical signals can be dispensed or acquired by a single needle. For addressing these limitations, microneedle devices often consist of arrays of needles. The total number of microneedles in a functional patch or device can change from a single needle to thousands of needles in array configurations (Birchall 2006; Sammoura et al. 2007). For making such arrays, a variety of micromanufacturing methods are available. Wilke et al. (2005) produced silicon microneedles via wet silicon etching and lithography which are widely used in microfabrication. Ovsianikov et al. (2007) presented the capability of two-photon polymerisation for making microneedles with small features including 20 μm wide pockets on the needle shaft. Tarbox et al. (2018) discussed the advantages and capability of silicone casting methods where high precision and cost-effectiveness can be achieved. Although these techniques allow the creation of complex microneedle geometries, most of them are not suitable for upscaling and are laborious processes. The unit cost, repeatability and elimination of batch processing steps should be considered while addressing a high-volume manufacturing scenario. From that perspective, a detailed review by (Juster et al. 2019) demonstrates the suitability of thermoplastic materials for microneedle manufacture using hot embossing, injection and micro-injection moulding where the suitability and cost-effectiveness are key benefits.

We have noticed that there is an unconscious misuse or misunderstanding regarding the usage of the term “micromoulding” in the literature from manufacturing and materials processing perspective. For instance, Tarbox et al. (2018) discusses the main features of silicone casting process where the micromoulding term is widely being used for casting of drug incorporated polymer solutions into the microneedle moulds made of Polydimethylsiloxane (PDMS). The process mentioned is a manual, lab-scaled casting method and encompasses three main steps including master mould and negative mould

making followed by the pouring of the polymer solution as generalised by Bediz et al. (2014). Needless to say, although this method provides a decent way of rapid prototyping for different polymeric microneedle formulations and widely used by the microneedle research community, the process is far from capable of up-scaling and is a manual process without the capability of automation. As far as the cost effectiveness, mechanical properties and manufacturing convenience are concerned, injection and micro-injection techniques are appropriate candidates for producing solid microneedle arrays in high throughputs using polymers.

Micro-injection moulding or simply "micromoulding" we refer in this work is a single-step, net-shape forming process for economical manufacture of miniature 3D products with high volumes, low marginal costs and high precision as demonstrated by Whiteside et al. (2003) and Whiteside et al. (2005). Excellent micro and nano feature replication capabilities of this manufacturing technique also has been proved in the recent years by the work from our group done by Nair et al. (2015) and Romano et al. (2019). These reports demonstrate that this technique is an ideal candidate for producing microneedles in a mass production scale alongside with their cleanroom environment option and automated, non-human contact manufacturing capability. The downside of the high capital costs of this manufacturing technology is mitigated by its high repeatability, short cycle times and the advancement in mould manufacturing technologies that reduce the mould making costs.

Laser micro-machining has become a prominent method for making micro & nano scaled functional surfaces on mould steels as discussed in our recently published work by Romano et al. (2019). Capabilities of laser milling/machining have been previously evaluated by Dimov et al. (2011) where nano and picosecond laser sources have been used on a stainless steel for creating microneedle cavities. The work proved that solid microneedle cavities can be machined solely by means of laser milling without the need of additional advanced

machining technologies on mould steel surfaces. This is an important feature that would make the microneedle process chain much simpler with less steps, yet flexible, since different prototype moulds, machining strategies and microneedle configurations can be manufactured using laser micro-machining. Very recently, Evens et al. attempted to present a novel method for making microneedles from thermoplastics using a state-of-the-art laser micro-machining system and injection moulding (Evens et al. 2020). The authors used a femtosecond laser source and were able to achieve tip radii as low as 3.75 μm with microneedle cavity depths changing between 1000 – 2000 μm. The report clearly shows that the usage of femtosecond laser pulses with recent advancements in optics and laser technology provides excellent machining capability for making microneedle moulds.

It is our aim in this work to combine the state-of-the-art of laser machining and micromoulding for microneedle manufacturing in a multi-process advanced manufacturing paradigm and to present a complete cost-effective process chain for solid microneedle arrays micromoulded from thermoplastic materials. The process chain includes mould making, micromoulding, in-line process data collection & interrogation and quality assessment of the microneedles. One of the main focus of this work is the evaluation of the micromoulding process and discuss whether in-line collected data can be used for quality assessment procedures for microneedles. The methods that we present here will prove that the micro-injection moulding process is the most suitable technique for high-volume manufacture of solid microneedle arrays. Our multi-process manufacturing paradigm and quality assessment steps of microneedles are schematically summarised in Fig. 1.

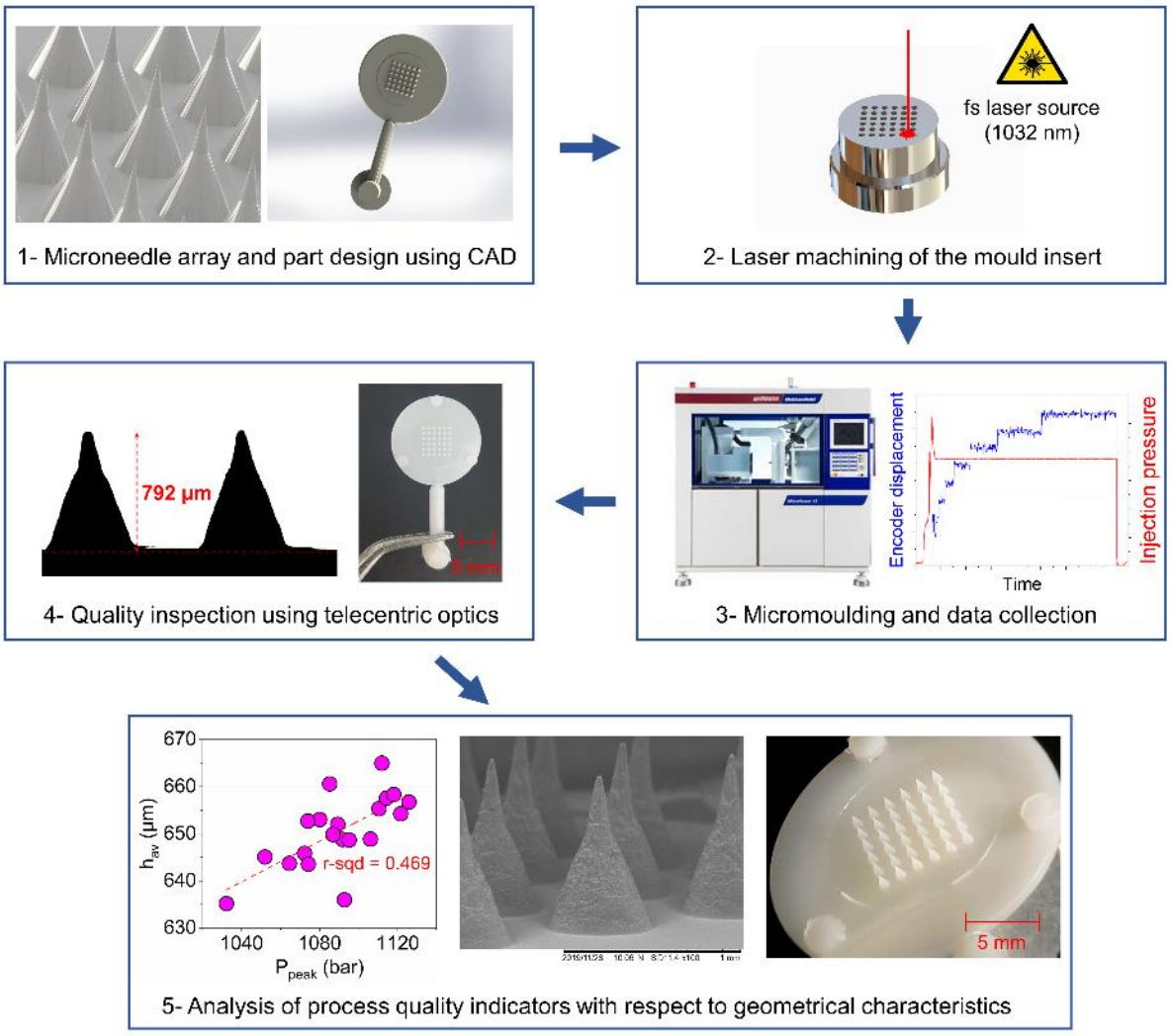

Fig. 1. Schematic showing different steps of our multi-process advanced manufacturing paradigm for microneedles.

Microneedle manufacturing process chain

Microneedle cavity and mould design

Microneedles can be fabricated for different types of delivery or monitoring methods such as dissolvable needles, coated needles, or simply in solid configuration for making pores on the skin. One of the most commonly used microneedle design is the latter because of their compatibility for different range of applications including poke & patch approach, dissolvable needles and also body condition-monitoring applications as covered by Larrañeta et al. (2016) and Mahony et al. (2019) respectively.

The cavities to be laser machined in this work were designed to have a solid body and a depth of circa 900 µm with 630 µm base diameter with a conical shape (see Fig.2). A square 6x6 microneedle array has been adopted in the mould insert design for microneedles. The first reason for this is the convenience of having a square array of needles during the quality inspection under the telecentric optical system. Secondly, as far as the skin permeabilities are concerned, hexagonal arrays only have a slight advantage over the square configuration as reported by Davidson et al. (2008). Another important consideration in array design is pitch distance where needles with smaller distances trigger a so-called "bed-of-nails" effect. This results in higher penetration forces since the pressure exerted by each needle tip will not be enough to penetrate the skin. The microneedle array used in this work has been designed with a 1 mm pitch distance, which was experimented previously by our group with another microneedle geometry by Nair et al. (2015). Al-Qallaf and Das (2009) discussed the importance of pitch distances between microneedles in an array and also found out that 1 mm distance is appropriate.

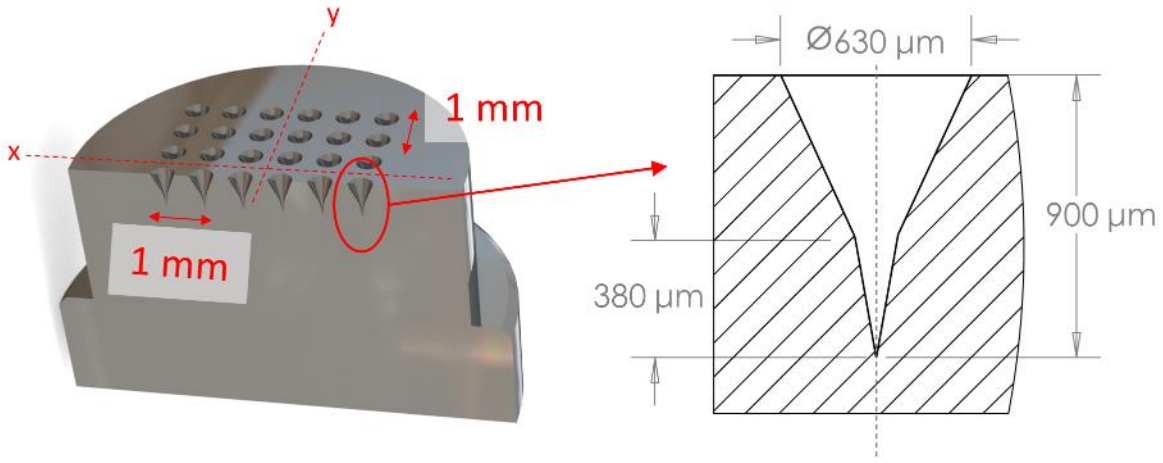

Fig. 2. Images depicting the cross section of the mould insert and dimensional features of the microneedle cavities. No dimensions for tip radius is given since it is determined as a result of the laser micro-machining and subsequent micromoulding processes. Notice that the pitch

distance in both directions in the microneedle array is 1 mm. Symmetry axes have been indicated with dashed lines.

It is of vital importance to consider the tip radii of the needles, not only for their impact on the functionality but also from a manufacturing perspective. Sharper needles that have radii approaching 1 μm can be very difficult to handle as the tips become extremely deformable and breakable. Davis et al. (2004) reported that solid microneedles with tip radius of 30 μm were sufficient to penetrate the human hand skin with relatively low insertion forces circa 1.3 N. The authors also concluded that insertion forces decrease linearly with the decreasing tip radius. Another more recent work by Champeau et al. (2020) focusses on pencil-like dissolvable microneedles with circa 15 μm tip radius according to their optical images. It was shown that the needle tips were sufficiently sharp to penetrate *ex-vivo* rat skins and 0.17 N / needle insertion force had been estimated. These reports signify that even tip radii as blunt as 30 μm have been sufficient for decent penetration of needles to the skin. However, decreasing the radius as low as possible will result in easier penetration and the patches will be less likely to induce pain. The ideal lower limit for tip radius of a microneedle can be approximated with the current technological limits of micromoulding where thermoplastic needles with 10 μm were successfully demoulded recently by (Evens et al. 2020).

A mould cavity plate with a straight runner and circular base with a diameter of 17.5 mm has been manufactured out of P20 tool steel (see Fig. 3). The cavity plate can accommodate interchangeable mould inserts in the middle with a diameter of 10 mm (see Fig.3a and c). The main circular cavity has been designed to have a 0.5 mm depth to provide a stable base for the microneedles (see Fig. 3a and b). The mould tool was made in Hasco K-standards and both fixed and moving halves of the tool accommodates a pair of 400 W cartridge heaters and J-type thermocouples to control the mould temperature. The mould tool

allows the flexibility to manufacture different configurations of microneedles in the same environment with minimal effort with the interchangeable insert capability.

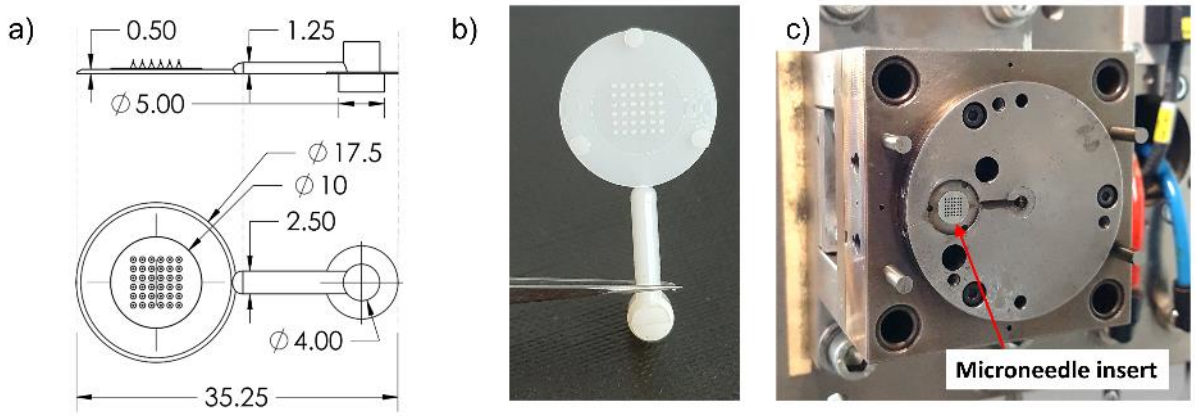

Fig. 3. Figure showing the part dimensions and mould design: a) Dimensions of the part, b) a real image of a moulded part, c) an image of the moving half of the mould tool. The laser machined insert is located in the centre of the circular cavity. All dimensions are in mm.

Laser micro-machining of the mould insert

A circular, button-type mould insert have been machined from a bar of Stavax ® ESR (Uddeholm). The material is widely known to be well-suited for injection moulding applications with its very good polishability, machinability and wear resistance. The surface of the mould insert had a 10 mm diameter and has been mechanically mirror-polished for obtaining a flat surface with no machining marks from the previous turning process.

The laser micro-machining of microneedle cavities in the present work has been carried out similarly to our previous study by Gülçür et al. (2020), where the toolpath was generated using a custom-built postprocessor within the CAD/CAM software (ArtCAM Autodesk). A femtosecond laser (Satsuma – Amplitude Laser) integrated into a multi-axis machining system (LASEA SA) was used to produce the microneedle cavities. A layer-by-layer machining strategy has been adopted in an x-y raster scanning mode which was rotated at 45° with respect to the previous layer (see Fig.4). The thickness of each machined layer

was approximately 1 µm and the focal plane for each layer was set by employing the Z-module of the 3D scanning head (RhoThor RTA Newson). The laser micro-machining parameters are summarised in Table 1.

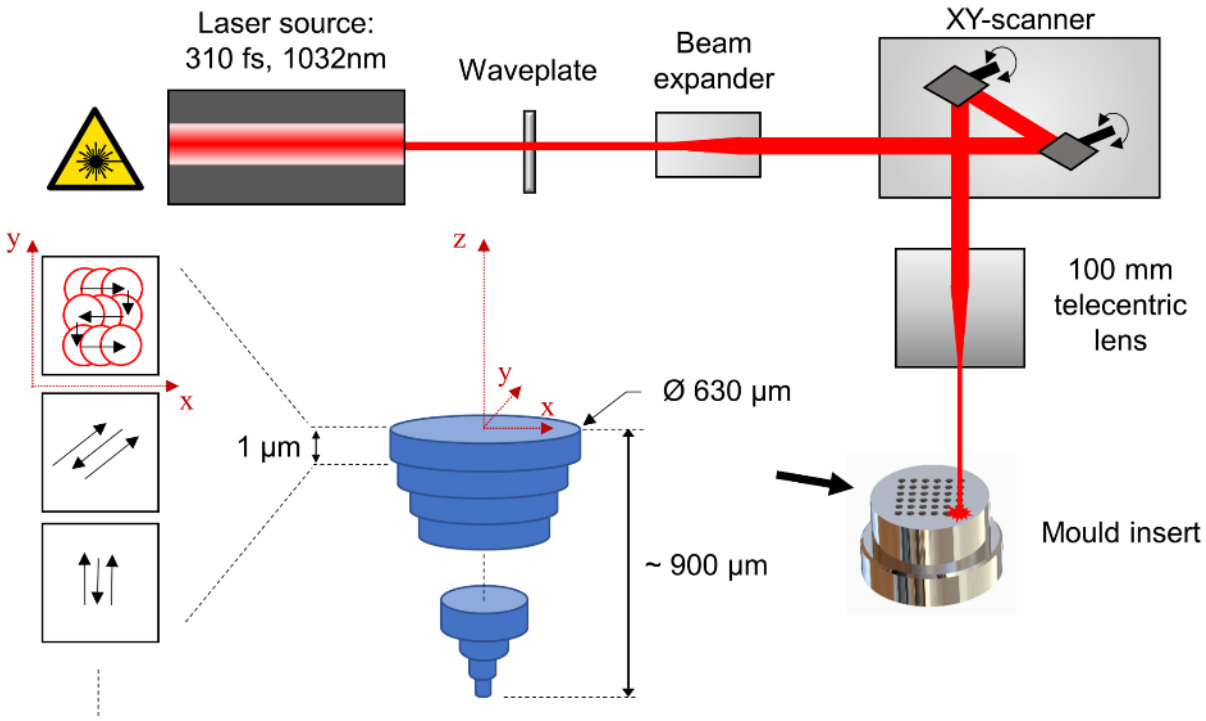

Fig. 4. A schematic depicting the laser micro-machining setup and the layer by layer scanning strategy. Note that the dimensions are not to scale.

Table 1. Laser machining parameters used for producing microneedle cavities.

Parameter	Value & units
Laser wavelength	1032 nm
Average laser power	3.5 W
Pulse duration	310 fs
Pulse repetition rate	500 kHz
Scanning speed	2000 mm/s
Beam spot diameter	30 µm
Scanning hatch distance	4 µm
Ablated thickness per layer	1 µm

Micromoulding process details

The equipment used in this work for replicating the microneedle mould cavities was a Wittmann-Battenfeld Micropower 15 state-of-the-art micromoulding machine. The machine has been designed to have a very precise closed-loop feedback system to control the injection pressures for filling very small micromoulding cavities. The closed-loop control of the pressure during the injection mitigates the variations that might arise from the dosage and is the most advanced controlling method of a micromoulding process. The plasticising unit of the machine is attached to the main injection channel at a 45° angle and incorporates a 14 mm plasticising screw for industry standard pellets. An injection piston with 5 mm diameter has been used to inject the molten polymer that is transferred from the dosing unit.

The thermoplastic material used in the present study was a commercial Acrylonitrile butadiene styrene (ABS) resin (CYCOLAC - HMG94MD, Sabic). This particular material was chosen because of its excellent flowability, suitability for thin walled medical applications and biocompatibility. The amorphous structure of the polymer was also an important consideration where the shrinkage values are relatively low (0.5 – 0.8%) as compared with semi-crystalline polymers. Typical physical properties of the ABS used are given in Table 2. The glass transition temperature of the material was determined using a differential scanning calorimetry (DSC) method at a 10°C / min heating rate.

Table 2. Physical properties of Sabic CYCOLAC - HMG94MD ABS resin.

Properties	Value & units
Melt Flow Rate, 220°C/5.0 kg	11.7 g/10 min
Tensile strength at yield	46 MPa
Glass transition temperature	106.7°C
Shrinkage	0.5 - 0.8 %
Density	1.06 g/cm³

Micromoulding experiments were designed in two main sets. The first set (Set1) of experiments was designed to have reasonable replication quality of the microneedle cavities, with lower switch-over and packing pressures than the ideal. The purpose of this was to monitor and investigate the inherent process characteristics of the manufacturing environment. The second set (Set2) of experiments use the highest pressure values possible to maximise microneedle replication, where the overall look of the parts are free from flashing effects and of good quality. Table 3 summarises the process settings used for the initial set of experiments (Set1) and manufacturing runs (Set2).

Table 3. Micropower 15 moulding parameters for making microneedle components.

	Melt temperature (°C)	Mould temperature (°C)	Injection velocity (mm/s)	Switch-over pressure (bar)	Packing pressure (bar)	Packing duration (s)
Set1	235	60	400	700	750	7.5
Set2	235	60	400	1050	1100	7.5

20 parts have been collected for both sets of experiments. Parts for both sets were sampled after 50 mouldings have been produced and discarded in series before collecting the actual samples for analysis. The reason for this is to stabilise the temperature gradients in the parts of the machinery, minimise frictional effects, and mimic a production scenario as close as possible.

In-line process monitoring of micromoulding

The Micropower 15 in this study is equipped with a range of output channels and sensors for data collection during micromoulding cycles. Available data include injection pressure, injection piston position, and cavity pressure measurement which are captured using

an ethernet-based National Instruments cDAQ – 9185 with NI-9215 modules. An analysis of the process data was carried out by extracting process quality indicators or proxies from the recorded data in relation to the dimensional or functional features of the parts. For instance, work published by Baruffi et al. (2018) report linear correlations between the integrals calculated from injection pressure data and critical dimensions of a part having a mass of 0.1 mg. The work is based on a design of experiments approach rather than a cycle-by-cycle analysis that make it difficult to consider in a wider manufacturing concept. Whiteside et al. (2005) also collected and analysed injection and cavity pressure data for assessing the process variations in a micromoulding production run. The authors indicate that the process variation increases with smaller micromoulding cavities and in-line quality assurance methods become critical for preventing defective parts to reach end users. No reports on in-line quality assurance procedures for microneedle manufacturing using injection or micro-injection moulding have been found in the literature. Because of its relevance to the micromoulding process quality, injection pressure has been selected as a datum for the present work and analysed in detail for a prospective in-line quality assurance scenarios for thermoplastic microneedle arrays. Position data coming from the encoder of the injection unit were also used in this work as it is complementary for the interpretation of the pressure data and for identifying the packing behaviour of a micromoulding process.

The injection pressure measurements were done using the built-in strain gauge sensor (X-Sensors XB 120-1500) on the machine which is located behind the injection piston. The output voltage (0 – 10 V) of the sensor was calibrated using a two point calibration according to the values recorded from the machine software (Unilog B8). The position data coming from the servo encoder were also calibrated using an external laser displacement sensor in a two point basis. A PC-based data collection suite incorporating a custom LabVIEW script

was created and multiple channels of data were recorded for each individual part produced. 100 Hz acquisition rate was used for capturing the micromoulding process data.

Fig.5 shows a typical micromoulding process data captured from a single cycle. The blue curve representing the piston displacement is a useful tool for following and identifying different stages of the process. Likewise, the corresponding changes in the injection pressure can be traced from the red curve, where a pronounced peak is seen at about t = 6.67 s. With a pre-defined injection specific switch-over pressure (see Table 3), the control system monitors the pressure build-up during the injection phase and piston decelerates where the unit goes into a pressure controlled packing phase from a velocity controlled injection. The reaction time for the control system is 20 μs, but the considerable amount of momentum in the injection piston movement means that it takes a small amount of time for pressure control to stabilise and a pressure overshoot over the set switchover value is often witnessed. The following plateau after the switch-over point in the injection pressure is the holding or packing phase that lasts for 7.5 s during which the shrinkage effects are compensated while constant pressure is applied. Points of particular interest here are defined as the injection pressure peak (P_{peak}), which is the peak value just after the the switch-over is carried out. P_{peak} can be an important quality indicator of the process as the magnitude of the pressure overshoot gives insight on how the control system of the machine responds to the monitored pressure values for switching-over to the packing phase. The parameter also contains information regarding how the injection unit is decelerated and has been previously used in the literature as a process quality indicator (Whiteside et al. 2005; Baruffi et al. 2018). P_{peak} values are monitored and recorded for each manufactured part individually on a cycle-by-cycle basis. LabVIEW codes are created to ensure that the extraction process of the quality proxies selected are standardised and automated in a pilot production scenario.

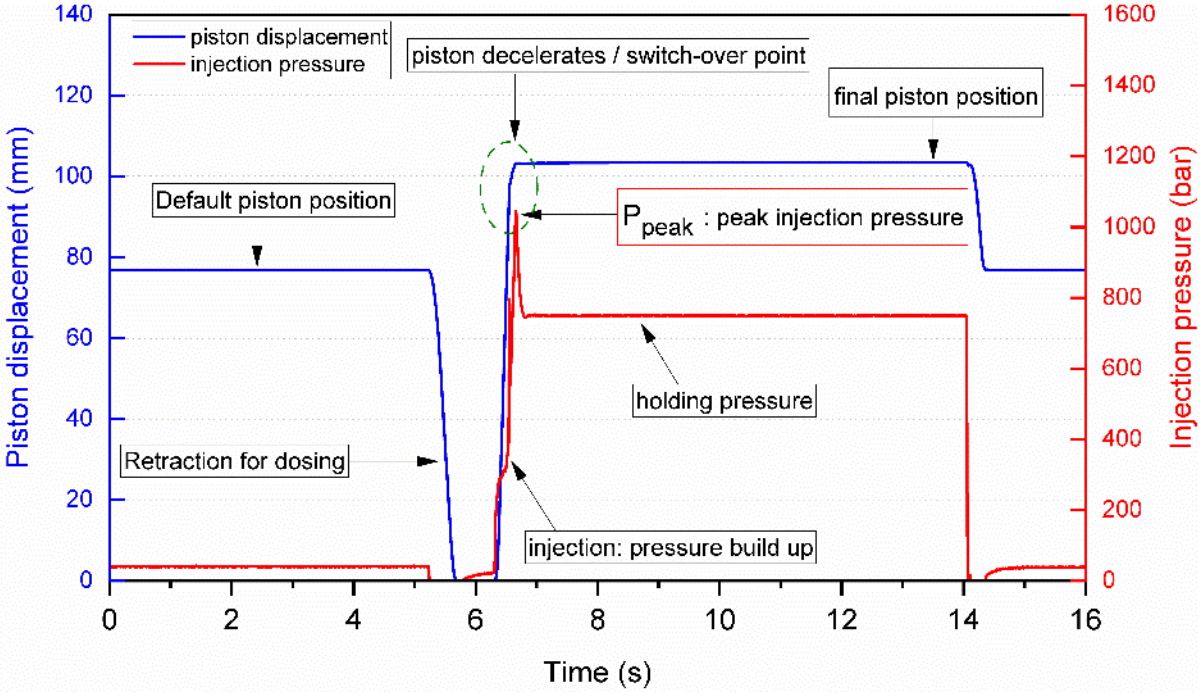

Fig. 5. Process data captured from a single micromoulding cycle of Micropower 15. The important features of the data are indicated.

Microneedle quality assessment

The quality assessment stage of the microneedle arrays have been reported to be a significant challenge when making prototypes or manufacturing microneedles in high volumes. The reason for this is the unsuitability of the microscopic techniques used by the researchers such as scanning electron microscopy, confocal microscopy and other conventional optical microscopy techniques in manufacturing environments (Waghule et al. 2019). Although these can provide more than sufficient capabilities in 3D assessments of the individual needles, it is literally impossible to use them for hundreds of thousands or even more individual needles due to their slow acquisition speeds. This is a commonly discussed bottle-neck aspect of micro and nano manufacturing where fast, yet accurate and easy to implement metrology solutions must be tailored for zero-defect production of miniature devices as discussed by Tosello et al. (2019). To address and tackle these challenges, a

bespoke quality inspection apparatus have been developed that can carry out the microneedle replication quality assessment. The quality inspection apparatus discussed here (see Fig. 6) is set up on the basis of telecentric imaging and machine vision at microscopic scales (<1 mm).

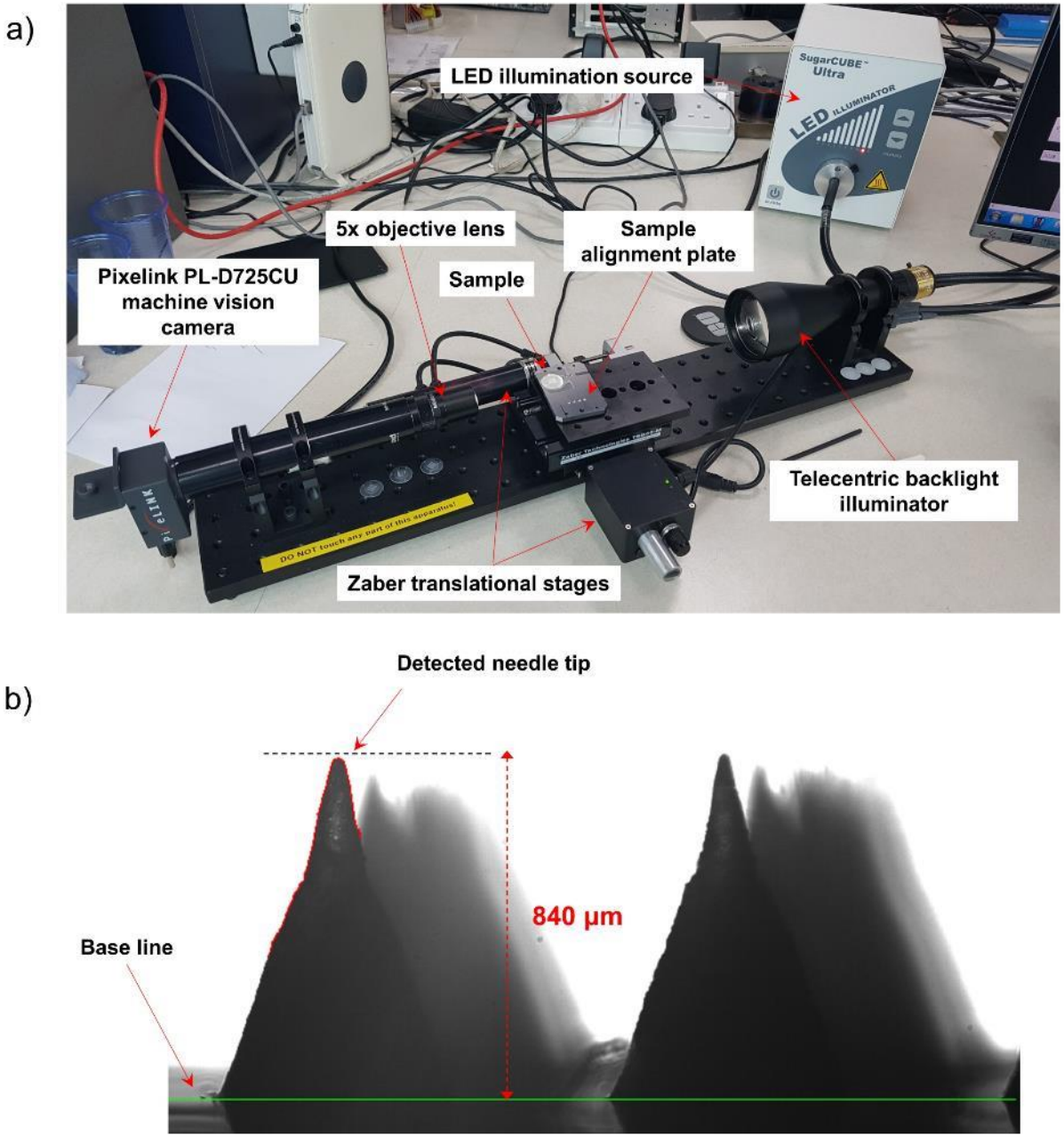

Fig. 6. Microneedle inspection system: a) Components of the telecentric imaging apparatus; b) a telecentric image showing the main measurement features.

Fig. 6a shows the main components of the measurement system. A machine vision camera (Pixelink PL-D725CU) captures the shadow images of the needles on the imaging side which

are put in the middle of the optical train between the camera and the telecentric backlight illuminator. A 5x telecentric objective lens was used for focussing the image onto the sensor of the camera. The CMOS device is capable of capturing images with a 5.3 megapixel resolution with a frame rate of 75 Hz. Two translational stages (Zaber Technologies) that move in x and y-axis facilitate the focussing of the camera on 36 individual needles on the replicas. Microneedles are aligned at 5° with respect to the axis normal to the main optical axis for calculating dx and dy values that are being used for the translational stages. This facilitates imaging and focussing of each individual needle in the optical axis. The system has been calibrated via a 5x graticule target by using pre-defined 1 mm measurement lines. The measurement principles can be seen in Fig.6b. A bespoke LabVIEW based software has been created ensures the individual needle to be characterised is focussed within a small depth of field. Edge detection is performed on the boundary edges of the 2D image of the needle, and the tip of the needle is determined to be the pixel in the edge detect result that is closest to the upper image border. The coordinate values of the needle tip pixel and a baseline at the substrate are then combined to determine needle height. The tip radius is calculated by applying a circular curve fit to a range of 7 pixels centred on the needle tip pixel.

The system allows inspection of 36 needles (1 part or cycle) in only 2 minutes and is currently limited by the comparatively slow stage movement. This is significant from metrology perspective since it usually takes hours to obtain a 3D image of the microneedles under a confocal microscope. With this setup, quality-related responses or dimensional product fingerprints of the microneedles can be extracted and analysed in conjunction with the collected data for process interrogation and variation analysis.

Results and discussion

Assessment of laser machined cavities

The layer-by-layer laser processing of the mould insert resulted in double-tapered microneedle structures with varying angles (~15°) towards the bottom of the microneedle cavity (Fig.7). The obtained cavity geometry is important from product design point of view since a wider base will provide the necessary mechanical stability and prevention of rupturing of sharp needles from the substrate. Moreover, the taper of the cavity narrows down at around 550 μm, which will allow the microneedle array to penetrate the skin only in a depth of approximately 350 μm due to the sharpness of the upper section of the needles.

The observations during the machining process of the microneedle insert showed that it took approximately 66 s to machine a single microneedle cavity. Hence, a total machining time of circa 40 minutes has been recorded for the creation of 36 needle cavities on the mould insert. This is a remarkably short machining time for such microstructures when compared with other state-of-the-art mould making methods. One good example would be micro-electrical discharge machining (micro-EDM), which is a widely used technique for producing micro-tooling cavities and machining microstructures that has machining times which are much longer for aforementioned geometries (Nair 2014). Using micro-EDM requires the preparation and dressing of the electrodes multiple times for machining relatively deep microneedle cavities. This makes the micro-EDM a labour-intensive and slow process where the preparation time of a microneedle mould insert will be at least two or four fold longer than laser micro-machining. Short machining times makes laser micro-machining a highly capable method for also rapid prototyping as different microneedle structures (shorter, longer, blunt etc.) can be experimented easily and cost-effectively.

It has been a particular challenge to evaluate the depth of the laser machined cavities with conventional microscopic techniques. The state-of-the-art focus variation and confocal microscopes usually suffer from a relatively small depth of focus in the z-axis and multiple

reflections on the side walls for deep microstructures. Hence, a silicone (Polydimethylsiloxane – PDMS) replication method was used for making a silicone replica of the mould features using a commercially available resin (Sylgard 184 – Dow). This particular material has been known for its high tensile strength, superior elastic recovery, and low shrinkage (1.1%) (Gale et al. 2008). The cured replica was then put under the telecentric optical measurement system and a scanning electron microscope (SEM - Hitachi – TM3000) for the evaluation of the cavity depths. Fig.7a and b shows the images of the PDMS replica and replicated mould cavities, respectively. The telecentric image shown in Fig.7b depicts the main features of the produced cavities with very sharp tips. The mould insert was also inspected with SEM in order to investigate the machining quality of the side walls of the cavities (Fig. 7c). The SEM image show that despite having a low depth of focus, the base of the cavity has been machined isotropically owing to the circular polarisation of the laser beam. The SEM image shown in Fig. 7d was taken from the PDMS replica and it can be seen that the narrower taper has a slightly better surface finish than the base of the needle. This can be attributed to a phenomenon called plasma shielding during the laser micro-machining process as suggested by Evens et al. (2020) where a combination of vaporised material and plasma formation leads to a shielding effect for the laser beam after a certain depth. As a result, the point where the laser is focussed changes and features that are smaller than the laser spot size can be machined with relatively better surface finish.

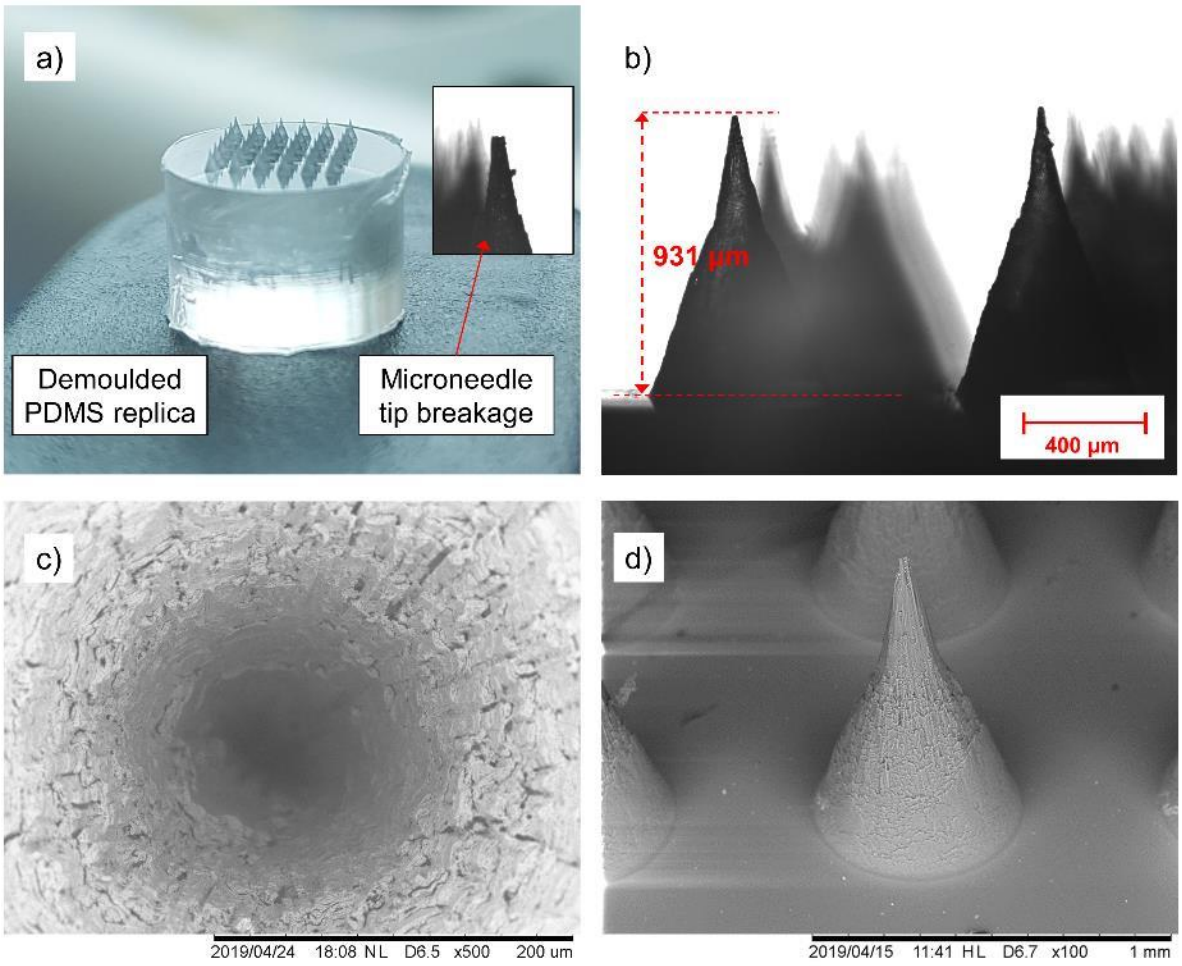

Fig. 7. The PDMS replica: a) a close up image of the replica; b) a telecentric image showing an example measurement; c) an SEM image depicting the machining marks on the mould walls; d) an SEM image of a single PDMS microneedle.

Table 4 shows the measurement results obtained from the PDMS replica that were used for quantitative assessment of the machined cavities using the telecentric optical measurement system. The results show that an average cavity depth of 912 µm were achieved. For the assessment of repeatability of cavity machining and microreplication, a statistical parameter called coefficient of variation (CoV) has been calculated by dividing the standard deviations to the mean value of the measured entity. Statistically, CoV is more representative of the repeatability of the processes since it is normalised by the mean value.

Confidence intervals for CoV change significantly from application to application, however, it can be generalised that CoV values below 10% represent decent repeatability. A CoV value of 2.66% for machined cavities suggests a very good evidence of a repeatable machining process despite the fact that it is a thermal process. The average tip radius was found to be 5.2 μm, yet, with a CoV of 52.4% which is significantly higher than the needle height variations. This is expected due to the plasma shielding side effects when producing relatively deep cavities, especially towards the microneedles' tips. Moreover, the edge detection mechanisms used in the measurements also contributed to this high CoV. Additionally, it should be noted that a tip radii as sharp as 2 μm were also measured that shows what can be achieved with a state-of-the-art laser micro-machining system for producing of microneedle cavities with extremely sharp tips. Cleaning steps have been carried out for dissolving PDMS particles that can be present in the cavities after the demoulding procedure. The insert has been soaked in toluene for at least two days and sonicated in acetone for making sure that all remaining particles from the cavities were removed.

Table 4. Statistics obtained from the telecentric measurements of PDMS replica.

	Average (μm)	SD (μm)	CoV (%)	Max. (μm)	Min. (μm)
Cavity depth	912	24	2.66	952.	854
Tip radius	5	3	52.4	16	2

These results also suggest that the demoulding procedure of the PDMS replica can also be challenging. Cavity depths as low as 854 μm and a maximum tip radius of 16 μm indicate that these particular tips are very likely to be ruptured during demoulding. This implies that CoVs for cavity depth and tip sharpness can be even lower with a more controlled demoulding procedure for the PDMS replicas. Overall, the achieved cavity depth

and sharpness is more than satisfactory, since extremely sharp needle tips can become problematic while demoulding the parts after the micromoulding cycles.

Microreplication assessment

Each sample that had 36 microneedles were collected from Set1 and Set2 and inspected under the telecentric inspection apparatus. Two main product criteria were defined for the microneedle replication assessment. The first one is the average microneedle height (h_{av}) calculated for each replica with 36 needles. In a similar fashion, the average tip radius (r_{av}) was also calculated. Fig. 8 shows the results for h_{av} and r_{av} from these measurements.

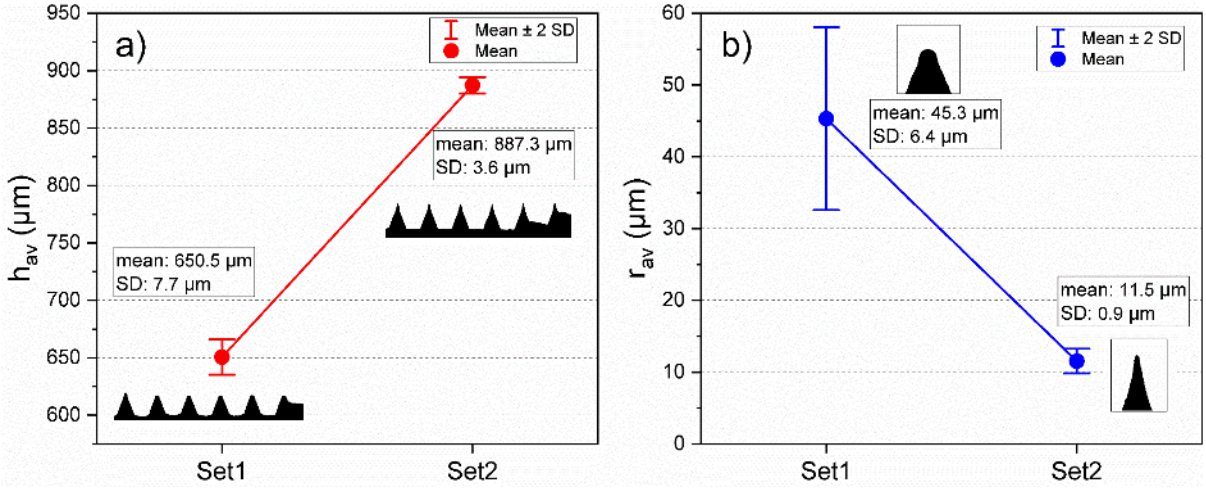

Fig. 8. Measurement results: a) the average needle height (h_{av}); b) the average tip radius (r_{av}) for Set1 and Set2. The standard error bars have a coefficient of 2x. Notice the representative telecentric images for particular sets.

The data in Fig.8a show that the increased pressure values used for Set2 resulted in significantly better replicas in terms of needle height. The h_{av} value of 887.3 µm for Set2 indicates that 97% of the microneedle cavities have been successfully replicated. Thus, it can be clearly stated that the elevated pressure in Set2 reduced the variations in product quality considerably.

The increase of the switch-over pressure from 700 to 1050 bar means that the deceleration of the injection unit was carried out slightly later, which led to a better packing of the needle cavities. This is due to the fact that more material was able to be conveyed due to later switch over and also the packing pressure applied in holding phase. The continuous monitoring of the pressure values shows that the switch-over pressure is of great importance for the complete replication of micromoulding cavities. The reason for this is that lower switch-over pressures will trigger the unit to decelerate early and thus leading to a lower replication performance. The higher packing pressure of 1100 bar in Set2 also contributes to better replication because of the amorphous nature of the polymer used, which is favourable in packing and shrinkage compensation to achieve better filling. The improvements from Set1 to Set2 are also evident from the standard deviation values. The CoV value of h_{av} in Set2 is 0.40% and this prove the highly repeatable aspect of the micromoulding process.

Similar results were achieved for r_{av} (Fig.8b), where the average tip radii as low as 12 μm has been obtained using higher pressure values. A CoV value of 7.8% for r_{av} in Set2 could suggest that the curve fit algorithm in radius detection might be influencing the measurements as it was close to the limits of the camera used. The greyscale intensities near the detected tips are the reason for this behaviour, where the points detected vary from sample to sample resulting in a bigger variation. Table 5 summarises the results obtained from the measurements.

Table 5. Statistical data for microneedle replication.

	h_{av} (μm)	CoV (h_{av}) (%)	r_{av} (μm)	CoV (r_{av}) (%)
Set 1	651	1.18	45	14.1
Set 2	887	0.4	12	7.8

For further investigation of some of the better ABS microneedle replicas from Set2, the samples were gold coated and inspected with SEM (see Fig. 9). The SEM micrograph in Fig. 9a show a well-replicated microneedle tip, with a radius down to circa 11 μm. The SEM image shown in Fig. 9b clearly depicts that all the laser machining marks have been well replicated from base to the tip of the microneedles.

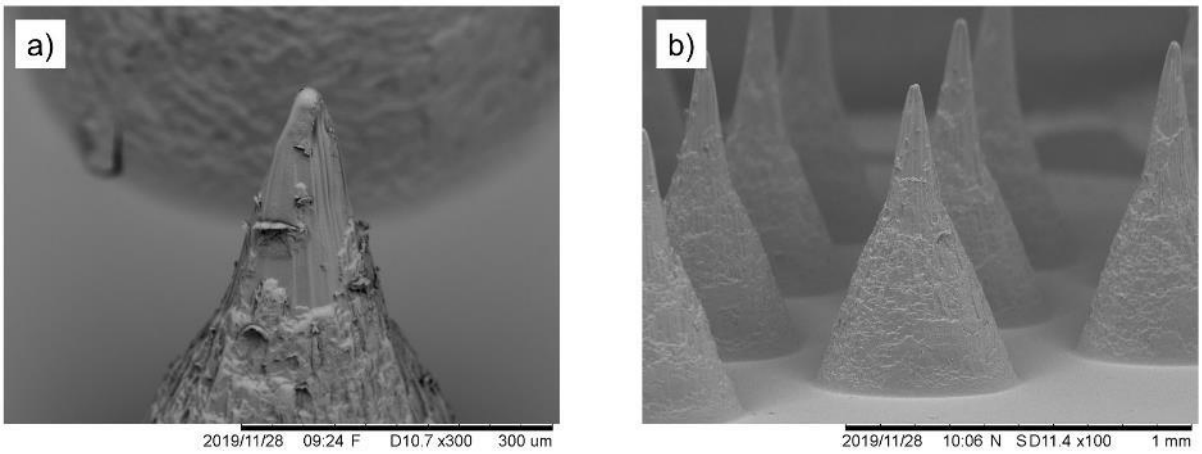

Fig. 9. SEM images of microneedles: a) a close-up image of the microneedle top; b) an image showing main features of the microneedles.

Process data analysis

Captured process data has been analysed to investigate the trends in product and process quality indicators, namely h_{av}, r_{av}. $P_{peak.}$ The data given in Fig.10 show that P_{peak} is an indication of well replicated microneedles where a minimum value of 1275.3 bar has been recorded for producing a part with h_{av} = 883 μm and r_{av} = 13 μm. It is also important that after this minimum P_{peak} value, there is higher variation of P_{peak} (SD = 218.4 bar) for Set2. The higher switch-over and packing pressures for Set2 ensure that the variations that can have an impact on microreplication performance are minimised to negligible values that cannot be detected and/or are insignificant. This is evident from the very low CoV value (0.4%) of h_{av} (see Table 5), which suggests that the process is very repeatable. An obvious positive linear trend between P_{peak} and h_{av} is also present in the sub-graph for Set1 where the increase of P_{peak} result in a better replication for the lower-end process parameters. However, r_{av} has shown a scattered behaviour for Set1 that is in agreement with the challenges associated with the measurement of the tip radii. The scatter plots also provide a visual depiction of the data given in Table 5, where the repeatability of Set2 values was presented. Overall, the data presented in Fig. 10 clearly show that the P_{peak} values obtained during the

switch-over can be reliable quality indicators where threshold values can be set accordingly. Hence, this "process fingerprint" can be used for quality assurance in a microneedle manufacturing platform based acquired injection pressure data. It is worth noting that the injection pressure data is being made available by the manufacturer of the machine as default and there is no need for additional sensors. This makes the injection pressure data a promising candidate for implementing cost-effective solutions for in-line quality assurance in microneedles' production.

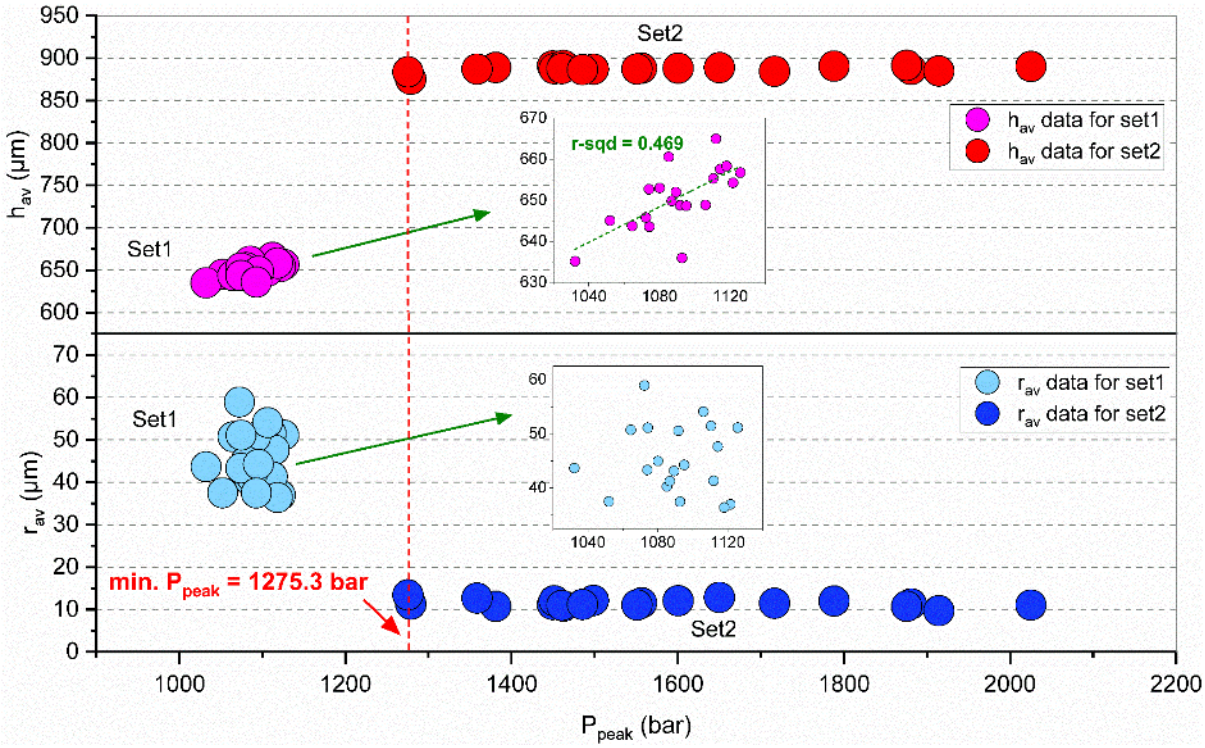

Fig. 10. Scatter plot showing the relationships between P_{peak} and product quality indicators. The sub plots show the scattered data obtained for Set1. Minimum P_{peak} for Set2 is indicated with red arrow.

The data collected can be used for pass-fail procedures or detection of the disturbances that occur during the manufacturing cycles such as heater failures, mechanical friction, or batch-to-batch changes in polymer viscosity as they can affect the injection pressures directly. The

encoder data indeed showed some interesting features (Fig. 5); however its low resolution (~60 μm) makes it less useful then pressure data when it comes to in-line quality detection. Attempts are being made to improve the resolution limitations in the position data by introducing high-speed laser displacement sensors for extracting more precise and relevant information.

Conclusions

A complete process chain for microneedle manufacture including part design, laser micro-machining of moulds, and micromoulding has been demonstrated alongside with extensive quality assessment and real-time process monitoring in this work. Considering the high costs of injection mould tool making which sometimes can be as expensive as the moulding equipment itself, the capability of laser micro-machining for producing microneedle cavities is significant. The total machining time of 40 minutes for a single mould insert is highly competitive with other industrial methods and very small tip radii (~2 μm) with good quality surfaces on the mould walls can also be attained. The CoV of 2.66% in achieving the desired depth of cavities also signify the repeatability and suitability of the process in a real manufacturing scheme, despite the fact that it was also negatively affected by the PDMS demoulding procedures. Another significant challenge was also addressed in microneedle manufacture by building a bespoke telecentric measurement system for efficient quality assurance. Measurement times as low as 2 minutes for a 6x6 microneedle array are significantly fast and can allow the users to create their own databases for microneedle replication for the assessing the suitability of selected manufacturing processes and detection of process variations. This new quality assessment capability of microneedles also implemented into an in-line quality assurance procedure where the quality criteria of the parts were analysed in conjunction with quality indication features referred as “process

fingerprints" taken from the in-house available machine sensor data. The initial results based on the injection pressure data have been promising and offer the capability for a real-time monitoring of the manufacturing cycles that can be implemented into robot-assisted pass-fail procedures and can prevent the manufacture of faulty parts.

Author contributions

Mert Gulcur: Conceptualisation, Methodology, Software, Investigation, Data curation, Writing – Original draft, Visualisation, Project administration. **Jean-Michel Romano:** Methodology, Investigation, Writing – Review & Editing, Visualisation. **Pavel Penchev:** Methodology, Investigation. **Tim Gough:** Conceptualisation, Supervision. **Elaine Brown:** Conceptualisation, Supervision. **Stefan Dimov:** Writing – Review & Editing, Funding acquisition. **Ben Whiteside:** Conceptualisation, Methodology, Software, Writing – Review & Editing, Supervision, Funding acquisition.

Acknowledgements

This research work was undertaken in the context of MICROMAN project ("Process Fingerprint for Zero-defect Net-shape MICROMANufacturing", http://www.microman.mek.dtu.dk/). MICROMAN is a European Training Network supported by Horizon 2020, the EU Framework Programme for Research and Innovation (Project ID: 674801). This research has also received funding and support from two other Horizon 2020 projects: HIMALAIA (Grant agreement No. 766871) and Laser4Fun (GA no. 675063).

REFERENCES

Al-Qallaf, B. and Das, D. B. (2009) Optimizing microneedle arrays for transdermal drug delivery: Extension to non-square distribution of microneedles. *Journal of Drug Targeting* 17 (2), 108-122.

Baruffi, F., Calaon, M. and Tosello, G. (2018) Micro-Injection Moulding In-Line Quality Assurance Based on Product and Process Fingerprints. *Micromachines* 9 (6).

Bediz, B., Korkmaz, E., Khilwani, R., Donahue, C., Erdos, G., Falo Jr, L. D. and Ozdoganlar, O. B. (2014) Dissolvable microneedle arrays for intradermal delivery of biologics: Fabrication and application. *Pharmaceutical Research* 31 (1), 117-135.

Birchall, J. C. (2006) Microneedle array technology: The time is right but is the science ready? *Expert Review of Medical Devices* 3 (1), 1-4.

Champeau, M., Jary, D., Mortier, L., Mordon, S. and Vignoud, S. (2020) A facile fabrication of dissolving microneedles containing 5-aminolevulinic acid. *International Journal of Pharmaceutics* 586, 119554.

Davidson, A., Al-Qallaf, B. and Das, D. B. (2008) Transdermal drug delivery by coated microneedles: Geometry effects on effective skin thickness and drug permeability. *Chemical Engineering Research and Design* 86 (11), 1196-1206.

Davis, S. P., Landis, B. J., Adams, Z. H., Allen, M. G. and Prausnitz, M. R. (2004) Insertion of microneedles into skin: measurement and prediction of insertion force and needle fracture force. *Journal of Biomechanics* 37 (8), 1155-1163.

Dimov, S., Petkov, P., Lacan, F. and Scholz, S. (2011) Laser milling: Tool making capabilities. *30th International Congress on Applications of Lasers and Electro-Optics, ICALEO 2011.* https://www.scopus.com/inward/record.uri?eid=2-s2.0-82655170859&partnerID=40&md5=fd97f2d2cf44ed6bed59c2c9b2dcdd17.

Evens, T., Malek, O., Castagne, S., Seveno, D. and Van Bael, A. (2020) A novel method for producing solid polymer microneedles using laser ablated moulds in an injection moulding process. *Manufacturing Letters* 24, 29-32.

Gale, B. K., Eddings, M. A., Sundberg, S. O., Hatch, A., Kim, J. and Ho, T. (2008) Low-Cost MEMS Technologies. In Gianchandani, Y. B., Tabata, O., and Zappe, H. (editors) *Comprehensive Microsystems.* Oxford: Elsevier. 341-378. http://www.sciencedirect.com/science/article/pii/B9780444521903000112

Gülçür, M., Brown, E., Gough, T., Romano, J.-M., Penchev, P., Dimov, S. and Whiteside, B. (2020) Ultrasonic micromoulding: Process characterisation using extensive in-line monitoring for micro-scaled products. *Journal of Manufacturing Processes* 58, 289-301.

Juster, H., van der Aar, B. and de Brouwer, H. (2019) A review on microfabrication of thermoplastic polymer-based microneedle arrays. *Polymer Engineering & Science* 59 (5), 877-890.

Larrañeta, E., Lutton, R. E. M., Woolfson, A. D. and Donnelly, R. F. (2016) Microneedle arrays as transdermal and intradermal drug delivery systems: Materials science, manufacture and commercial development. *Materials Science and Engineering: R: Reports* 104, 1-32.

Mahony, C. O., Bocchino, A., Haslinger, M. J., Fechtig, D., Schossleitner, K., Galvin, P. and Brandstätter, S. (2019) Characterisation of Microneedle-Based ECG Electrodes Fabricated Using an Industrial Injection-Moulding Process. *2019 IEEE 32nd International Conference on Micro Electro Mechanical Systems (MEMS).* 27-31 Jan. 2019.

Nair, K. (2014) *Micro-injection moulded microneedles for drug delivery*. University of Bradford.
Nair, K., Whiteside, B., Grant, C., Patel, R., Tuinea-Bobe, C., Norris, K. and Paradkar, A. (2015) Investigation of plasma treatment on micro-injection moulded microneedle for drug delivery. *Pharmaceutics* 7 (4), 471-485.
Ovsianikov, A., Chichkov, B., Mente, P., Monteiro-Riviere, N. A., Doraiswamy, A. and Narayan, R. J. (2007) Two photon polymerization of polymer-ceramic hybrid materials for transdermal drug delivery. *International Journal of Applied Ceramic Technology* 4 (1), 22-29.
Prausnitz, M. R. (2004) Microneedles for transdermal drug delivery. *Advanced Drug Delivery Reviews* 56 (5), 581-587.
Prausnitz, M. R. (2017) Engineering microneedle patches for vaccination and drug delivery to skin. *Annual Review of Chemical and Biomolecular Engineering* 8, 177-200.
Romano, J. M., Gulcur, M., Garcia-Giron, A., Martinez-Solanas, E., Whiteside, B. R. and Dimov, S. S. (2019) Mechanical durability of hydrophobic surfaces fabricated by injection moulding of laser-induced textures. *Applied Surface Science* 476, 850-860.
Sammoura, F., Kang, J., Heo, Y.-M., Jung, T. and Lin, L. (2007) Polymeric microneedle fabrication using a microinjection molding technique. *Microsystem Technologies* 13 (5), 517-522.
Tarbox, T. N., Watts, A. B., Cui, Z. and Williams, R. O., III (2018) An update on coating/manufacturing techniques of microneedles. *Drug Delivery and Translational Research* 8 (6), 1828-1843.
Tosello, G., Gulcur, M., Whiteside, B., Coates, P., Luca, A., De Sousa Lia Fook, P. V., Riemer, O., Danilov, I., Zanjani, M. Y., Hackert-Oschätzchen, M., Schubert, A., Baruffi, F., Achour, S. B., Calaon, M., Nielsen, C. V., Bissacco, G., Cannella, E., Rasmussen, A., Bellotti, M., Saxena, K., Qian, J., Reynaerts, D., Santoso, T., Syam, W., Leach, R., Kose, S. K., Parenti, P., Annoni, M., Cai, Y., Luo, X., Qin, Y. and Zeidler, H. (2019) Micro product and process fingerprints for zero-defect net-shape micromanufacturing. *European Society for Precision Engineering and Nanotechnology, Conference Proceedings - 19th International Conference and Exhibition, EUSPEN 2019.* https://www.scopus.com/inward/record.uri?eid=2-s2.0-85071006793&partnerID=40&md5=9d772fc9cd4e2b253918d15b3efd5dc9.
Waghule, T., Singhvi, G., Dubey, S. K., Pandey, M. M., Gupta, G., Singh, M. and Dua, K. (2019) Microneedles: A smart approach and increasing potential for transdermal drug delivery system. *Biomedicine and Pharmacotherapy* 109, 1249-1258.
Whiteside, B. R., Martyn, M. T., Coates, P. D., Allan, P. S., Hornsby, P. R. and Greenway, G. (2003) Micromoulding: Process characteristics and product properties. *Plastics, Rubber and Composites* 32 (6), 231-239.
Whiteside, B. R., Spares, R., Howell, K., Martyn, M. T. and Coates, P. D. (2005) Micromoulding: Extreme process monitoring and inline product assessment. *Plastics, Rubber and Composites* 34 (9), 380-386.
Wilke, N., Mulcahy, A., Ye, S. R. and Morrissey, A. (2005) Process optimization and characterization of silicon microneedles fabricated by wet etch technology. *Microelectronics Journal* 36 (7), 650-656.